

UPDATE ON MULTIPACTOR IN COAXIAL WAVEGUIDES USING CST PARTICLE STUDIO*

Gennady Romanov[#], Fermilab, Batavia, IL 60510, USA.

Abstract

CST Particle Studio combines electromagnetic field simulation, multi-particle tracking, adequate post-processing and advanced probabilistic emission model, which is the most important new capability in multipactor simulation. The emission model includes in simulation the stochastic properties of emission and adds primary electron elastic and inelastic reflection from the surfaces. The simulation of multipactor in coaxial waveguides have been performed to study the effects of the innovations on the multipactor threshold and the range over which multipactor can occur. The results compared with available previous experiments and simulations as well as the technique of MP simulation with CST PS are presented and discussed.

INTRODUCTION

A numerical simulation of multipactor became an essential tool to predict the multipactor regions for RF devices. There are a number of numerical simulation codes for predicting multipactor each with various pros and cons. Often these predictions are not in a full agreement with the experiments where the multipactor was observed. There are two common main reasons for this discrepancy. First, many of these simulation codes do not take into account energy distribution for secondary electrons and elastic/inelastic reflections with stochastic probabilities. Second, many codes use single-particle (macroparticle) approach which means that the information about the electron energy distribution and the statistical nature of electron reflection and emission are lost.

The inclusion of probabilistic electron reflection and secondary electron velocity distribution leads to the overlapping of the multipacting zones and broadens the range over which multipactor can exist. The theory behind this phenomenon has been discussed by many authors [1-7]. CST Particle Studio uses an advanced probabilistic emission model developed by Furman and Pivi [8]. Along with true 3D multi-particle tracking that makes CST Particle Studio powerful and sophisticated tool which can reveal more details.

Another important effect is so called ponderomotive or Gaponov-Miller [9] force, which tends to push charged particles towards regions of low field amplitude. This can have both a qualitative and a quantitative effect on the multipactor regions and definitely makes a difference for travelling and standing waves in coaxial waveguide. A series of simulations has been performed in this work in order to get better understanding what happens to the multipactor threshold in the case of a standing wave in coaxial waveguide.

MODEL USED AND SIMULATION TIPS

For modelling the 50 Ω coaxial waveguide with an outer diameter of 103 mm and inner diameter 44.8 mm used in the couplers for the SPL 704 MHz superconducting cavities was taken from [10]. Some simulations in this work were performed using a single-particle code and there are the results to compare with.

Each of the coaxial conductors is assigned with separate source of initial electrons. The electrons are uniformly distributed over the conductor surfaces; they have initial energy uniformly distributed over 0-4 eV range and initial uniform angular spread $\pm 45^\circ$. Later the parameters of secondary and reflected electrons are governed by the Furman-Pivi emission model.

For particle tracking CST PS uses RF fields calculated by eigenmode solver only. Normally eigenmode solver gives a standing wave solution. A travelling wave solution was found using periodic boundary conditions with proper phase advance

In this paper the averaged secondary emission yield per impact $\langle \text{SEY} \rangle$ [11,12] is used as an indicator of multipactor. By some reasons it is more convenient parameter than the exponential growth recommended by CST PS tutorial on multipactor simulation.

The prior study has shown no visible dependence of multipactor parameters on mesh density. This result contradicts the view that a reliable multipactor prediction requires very high mesh density. That is true if too small number of initial particles is used in simulations.

Using a small number of initial particles leads to a considerable stochastic fluctuation in the results which converge only with increasing accuracy of tracking in very fine fields. A sufficient large number of initial particles (6-10 thousands in this work) can generate a tremendous number of hits and secondary particles (up to several millions). That makes the average values very consistent in spite of not very smooth fields calculated with a mesh of modest density.

Of course, large number of particles requires powerful computers and long simulation times. Unfortunately, this brutal force approach seems to be the most reliable way to simulate multipactor in real cases.

TW SIMULATION

Effect of probabilistic emission model

This study was performed using CST PS to compare the simulation with the results of single-particle code RKpactor [10] and to observe how prediction of multipactor threshold evolves with improving of emission model.

*Work supported by US Department of Energy

[#]gromanov@fnal.gov

The RKpactor code uses the emission model taken from [2], but without elastic/inelastic reflections, since RKpactor is a single-particle code and cannot use complete distributed secondary emission model. Multipactor is identified in the code by the number of secondaries produced for a persistent (resonant) trajectory and growth of the electron current. If these reach user defined values a multipactor ‘event’ is recorded and the number of phases that give events is plotted versus power.

The first series of CST PS runs was performed with only true SEY function for copper without inelastic/elastic reflections to find agreement with RKpactor. But energy and angular spreads for true secondary electrons were in effect. The second series of runs was performed using complete Furman-Pivi emission model.

As can be seen in Fig. 1, the results of first series show several distinct multipactor bands at various power levels, which are in excellent agreement with RKpactor results. But the bands in CST PS simulations are smeared and overlapped, especially at low power, due to the initial energy spread of secondary electrons.

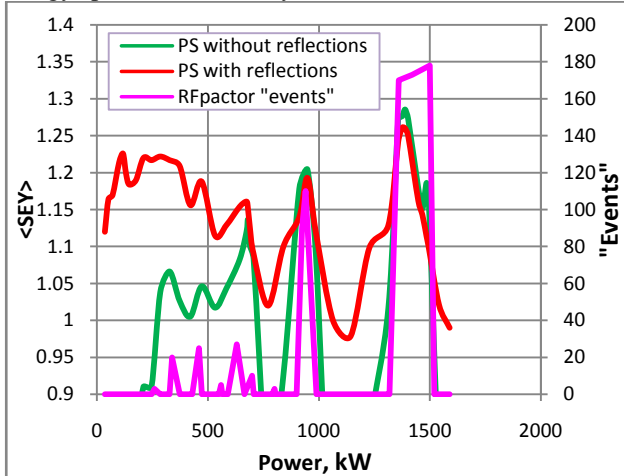


Fig.1. Comparison of CST PS and RKpactor simulations. CST PS is plotted against $\langle \text{SEY} \rangle$ and RFpactor is plotted against ‘events’ for various peak powers of electromagnetic wave. Peak SEY of 1.6 for copper was used in all simulations.

The results of second CST series also show the same multipactor bands above 500 kW, though they are merged even stronger. Additionally the results show a consistent multipactor below 500 kW with a curve similar to the SEY curve. This does not appear in the RKpactor results and in first series of CST PS simulations. Therefore this expansion of multipactor zone is due to the inclusion of elastic/inelastic electron reflection.

In general the low power multipactor is largely non-resonant, while high power bands are the resonant ones. So, both codes show the same results for the multipactor bands at high power, where the mass of trajectories are resonant. But for lower power end the single-particle codes do not find sufficient number of resonant trajectories to indicate multipactor and truncate multipactor zone.

Search of multipactor with reduced emission

Average $\langle \text{SEY} \rangle$ as a function of RF power has very important property – a similarity in respect to peak secondary emission of material. It means that if a true SEY peak value changes, then the $\langle \text{SEY} \rangle$ changes as shown in Fig.2.

The curves are similar and the potential multipactor zone is the same for each curve. So, a multipactor zone can be found at low values of peak SEY saving memory and dramatically reducing simulation time. But a statistically sufficient number of impacts should be provided to get the reliable results. It means that the number of initial and secondary electrons should be big enough.

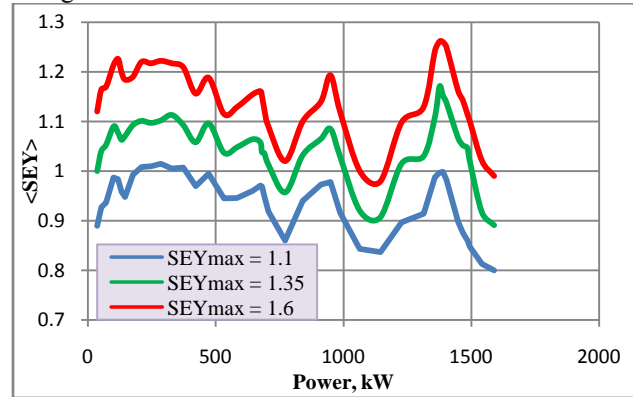


Fig.2. Average $\langle \text{SEY} \rangle$ as a function of power for different peak SEY values of material.

SW SIMULATION

In SW case the electric field amplitude has sinusoidal distribution and changes from zero to maximum. This implies a field gradient from field maxima to field minima. Due to the effect of the Gaponov-Miller force the electrons move along the waveguide towards the regions of lower field strength and get trapped there into electric field node area.

The effect of the Gaponov-Miller force was studied for mixed and standing waves in [13]. It was concluded that the multipactor threshold values strongly depend on the considered wave configuration, and the correlation between TW and SW thresholds is not that simple, contra to the results of [14]. But the most important conclusion made in [13] is that the multipactor can be mitigated for the SW configuration due to the attractor effect of the nodes of the SW pattern. The mitigation has been analysed numerically and confirmed in the experiment.

The detailed CST PS simulations performed for the chosen coaxial waveguide model confirmed this conclusion. But at the same time the simulations revealed in fact three different zones for multipactor in SW mode [15]. These zones can be seen in Fig.3, where $\langle \text{SEY} \rangle$ for both TW and SW are plotted versus RF electric field amplitude on the surface of the inner electrode, which is more appropriate parameter than the voltage between electrodes or RF power. Also average impact energy versus field level for SW case is shown on the same plot.

For low electric field up to 0.3 MV/m the CW multipactor exists, and it is similar to non-resonant multipactor for TW case (see Fig.4). Angular, velocity and energy spread of true secondary electrons along with high energy of the reflected electrons overcome the Gaponov–Miller force, which is not strong yet. So, there are enough electrons between the electric field nodes to support the discharge.

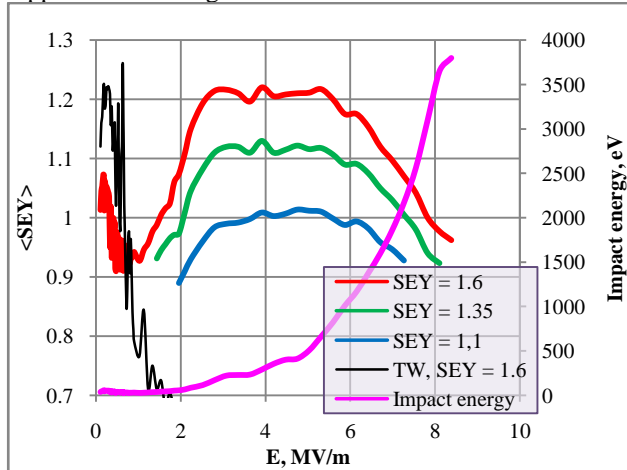


Fig.3. Average $\langle \text{SEY} \rangle$ for different peak SEY values of material and average impact energy versus electric field amplitude on the surface of inner electrode. $\langle \text{SEY} \rangle$ for TW is given for comparison.

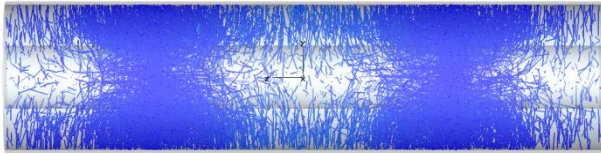


Fig.4. The snap-shot of the multipactor in standing wave for low electric field amplitude. The attraction effect of the Gaponov-Miller force is clearly seen.

In the medium field zone ($\approx 0.3 \div 1.0$ MV/m) the Gaponov-Miller force gains strength and all secondary electrons are eventually concentrated at the electric field nodes (Fig.5). There they cannot get a sufficient acceleration and the discharge dies down.

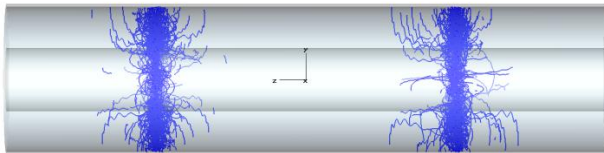


Fig.5. The snap-shot of the multipactor in standing wave for a medium electric field amplitude. The electron migration toward the field nodes is complete and the discharge is dying down.

For electric field amplitudes above 1.0 MV/m the concentration of electrons becomes even denser, but surprisingly enough the multipactor discharge restores. One can speculate about two reasons for that. First, the electrons oscillate around zero electric field nodes with amplitude, which remains finite even for very high electric field amplitude. The exact mechanism for that still should be understood better. But it is clear already

that the elastic/inelastic reflections are involved, since the multipactor does not occur without them at any field level. Second, the electric field in the interval of electron oscillations becomes high enough to initiate re-emission process.

In the simulations the multipactor at high field amplitudes is rather stable and persistent. But because of very small volume, where the discharge develops, the multipactor may be not very powerful in real coaxial devices.

CONCLUSION

Simulations of electron multipactor discharge in the coaxial waveguide have been performed using CST Particle Studio, with a primary goal to verify the effect of multi-particle approach combined with advanced probabilistic emission model on the discharge thresholds. Most simulations agree with analytical results and the results from more simplified numerical codes. It was confirmed and illustrated in details how incorporating an advanced emission broaden and merge the multipactor zones.

It was also confirmed that the multipactor for CW mode can be mitigated due to the effect of the Gaponov-Miller force. In addition to that it was found that at the electromagnetic field levels much higher than usual threshold for TW the multipactor can exist in the vicinity of the electric field nodes.

REFERENCES

- [1] V. Chernin, A. Drobot, and M. Kress, IEDM Tech. Dig., vol. 5, pp. 773–776, 1993.
- [2] V.P. Gopinath, J.P. Verboncoeur, and C.K. Birdsall, Phys. Plasmas, vol. 5, pp. 1535–1541, 1998.
- [3] L.V. Kravchuk et al, Proc. of Linac2000 Conf., Monterey, California, USA, 2000.
- [4] Grishin L.V. and Luk'yanchikov G.S., Sov. Phys. Tech. Phys. **21** 307–11, 1976
- [5] R. Seviour, IEEE Trans. on Electron Devices, vol.54, No 8, August 2005
- [6] A. Sazontov et al, Phys. Plasmas, **12** 053102, 2005
- [7] V.E. Semenov et al, Phys. Plasmas, **14**, 033509, 2007
- [8] M.A. Furman and M.T.F. Pivi. Physical Review Special Topics, Accel. and Beams, Volume 5. 2002.
- [9] A.V. Gaponov, M.A. Miller, Sov. Phys. JETP **7** (1958) 168.
- [10] G Burt et al, Proc. of LINAC10 Conf., Tsukuba, Japan, 2010
- [11] G.Romanov, Proc. of LINAC08 Conf., Victoria, Canada, 2008
- [12] G.Burt et al, Proc. of SRF2009 Conf., Berlin, Germany, 2009
- [13] Antonio M. Perez et al, IEEE Trans. on Plasma Science, vol.37, No 10, October 2009.
- [14] E. Somersalo, P. Yla-Oijala, D. Proch, and J. Sarvas, Part. Accel. **59**, 107, 1998
- [15] G.Romanov, Fermilab preprint FERMILAB-PUB-003-TD, 2011.